

Optimized shapes of oscillating resonators for generating high-amplitude pressure waves

Xiaofan Li^{a)}

Department of Applied Mathematics, Illinois Institute of Technology, Chicago, Illinois 60616

Joshua Finkbeiner^{b)} and Ganesh Raman

Department of Mechanical, Materials and Aerospace Engineering, Illinois Institute of Technology, Chicago, Illinois 60616

Christopher Daniels^{b)}

University of Akron, Akron, Ohio 44325

Bruce M. Steinetz

NASA Glenn Research Center, Cleveland, Ohio 44135

(Received 6 January 2004; revised 27 August 2004; accepted 5 September 2004)

Several studies have proved that the geometry of an oscillating acoustic resonator strongly influences its resonance frequencies and the nonlinear standing pressure waveform generated within the cavity. The research presented herein uses a quasi-one-dimensional numerical model to solve the acoustic field and is validated by comparing with experimental results. A quasi-Newton type numerical scheme is used to optimize the axisymmetric cavity contour by maximizing the pressure compression ratio, defined as the ratio of maximum to minimum gas pressure at one end of the oscillating resonator. Cone, horn-cone, and cosine resonator contours are each optimized for a fixed amplitude of the periodic external force oscillating the cavity. Different optimized shapes are found when starting with different initial guesses, indicating multiple local extrema. The maximum pressure compression ratio value of 48 is found in an optimized horn-cone shape. This represents a 241% increase in the compression ratio over any previously published results. © 2004 Acoustical Society of America. [DOI: 10.1121/1.1810139]

PACS numbers: 43.25.Gf, 43.25.Cb [MFH]

Pages: 2814–2821

I. INTRODUCTION

The waveform of the standing wave in an oscillating closed cavity is strongly influenced by the geometry of the resonator cavity. It is well known that shocks form in a cylindrical tube when the interior gas is oscillating at its resonance frequency. Lawrenson *et al.*¹ at MacroSonix Corp first exploited the shape dependence and obtained high-amplitude and shock-free acoustic pressures in axisymmetric tubes of varying cross sections, referred to as resonant macrosonic synthesis (RMS). Peak acoustic pressures that measure three to four times ambient pressure and maximum to minimum pressure ratios of 27 were observed in shaped cavities. The size of the demonstrated overpressure reached the level that is required by commercial applications such as acoustic pumps or compressors. The researchers considered these types of axisymmetric shapes: cylinder, cone, hone-cone, and bulb. They concluded that the hone-cone resonator shape generated the highest overpressure for a given input power. They also demonstrated that the overall characteristics of the waveform does not change when a resonator is filled with different gases.

A companion paper by Ilinskii *et al.*² developed a one-dimensional frequency-domain model for studying the RMS numerically. The results confirmed the nonlinear standing

waveform and the related characteristics such as shape-induced resonance hardening and softening observed in the experiments by Lawrenson *et al.*¹ To account for the energy losses in the boundary layer along cavity wall, Ilinskii *et al.*³ later modified the one-dimensional model by introducing an additional term in the continuity equation and used a turbulence model. Hamilton *et al.*⁴ analytically investigated the relationship between the natural frequency of a nonlinear acoustic resonator and its shape as well as the nonlinear interactions of modes in the resonator. Chun and Kim⁵ numerically investigated cosine shaped resonators in addition to cylindrical and conical shapes using high-order finite-difference approximations. They concluded that the half cosine-shape is more suitable to induce high compression ratio than other shapes under certain assumptions. Recently, Erickson and Zinn⁶ used the Galerkin method to solve the one-dimensional model and found a nonmonotonic increase in compression ratio when the flare constant is raised for a class of horn-shaped resonators. To serve commercial needs, such as in an acoustic gas compressor and an acoustic liquid pump, the objective is to find an optimized shape for generating the greatest overpressure. However, the optimization procedure and results have not yet been discussed.

In this article, the numerical schemes are introduced and the results are presented for optimizing the shape parameters that yield the highest maximum-to-minimum pressure ratio in each of the following resonator shapes: cone, horn-cone, and cosine-shape. In Sec. II, the modeling equations are pre-

^{a)}Electronic mail: lix@iit.edu

^{b)}Current address: NASA Glenn Research Center, Cleveland, Ohio 44135.

sented; in Sec. III, the numerical schemes are described; in Sec. IV, the numerical model and experiment results are compared and the resulting optimized shapes are discussed.

II. GOVERNING EQUATIONS

In the following section we briefly describe the one-dimensional model for computing the acoustic wave field in an axisymmetric resonator. The equations are presented for completeness and the details of the derivation are given in the work by Ilinksii *et al.*² The possible effects of the boundary layer along the resonator wall and the acoustically generated turbulence on the acoustical field are neglected in this model.

Consider the acoustic field in an oscillating resonator of length l driven by an external force. The resonator is axisymmetric with the inner radius given by $r=r(x)$, $0 < x < l$, where x is the coordinate along the axis of symmetry. The density of the gas ρ , the velocity u , and the pressure p satisfy the conservation of mass,

$$\frac{\partial \rho}{\partial t} + \frac{1}{r^2} \frac{\partial}{\partial x} (r^2 \rho u) = 0, \quad (1)$$

and the conservation of momentum,

$$\frac{\partial u}{\partial t} + u \frac{\partial u}{\partial x} = -\frac{1}{\rho} \frac{\partial p}{\partial x} - a(t) + \frac{(\zeta + 4\eta/3)}{\rho} \frac{\partial}{\partial x} \left(\frac{1}{r^2} \frac{\partial}{\partial x} (r^2 u) \right), \quad (2)$$

where $a(t)$ is the acceleration of the resonator enforced by the external force; ζ and η are coefficients of viscosity. Shear viscosity is denoted as η , and ζ is the bulk viscosity that results from nonequilibrium deviations between the actual local pressure and the thermodynamic pressure. The no-penetration boundary conditions at the two ends require that the velocity vanish at $x=0$ and l . The state equation is specified by that of an ideal gas,

$$p = p_0 (\rho/\rho_0)^\gamma, \quad (3)$$

where p_0 and ρ_0 are the ambient pressure and density, respectively, and γ is the ratio of specific heats of the gas.

The quasi-one-dimensional compressible Navier–Stokes equations (1)–(3) are solved using a frequency-domain method, where the unknown variables are expressed in terms of finite Fourier series in time. The Fourier coefficients are determined using a shooting method. Both the experimental and numerical results show that the time harmonics of the dependent variables, such as the pressure p , decay rapidly as the frequency increases. This ensures that the number of time harmonics, N , needed for accurate results is small. In the present numerical simulations, the value of N is twenty and it can be shown that increasing N does not change the results.

Following Ilinksii *et al.*² by expressing the variables in Fourier series, Eqs. (1) and (2) can be reduced to a system of

Ordinary Differential Equations (ODEs) for the Fourier coefficients of the velocity potential φ , defined as $u = \nabla \varphi$:

$$\frac{d\hat{\varphi}_k}{dx} = \frac{\hat{v}_k}{r^2}, \quad \text{for } k=1,2,\dots,N, \quad (4)$$

$$\sum_l D_{kl} \frac{d\hat{v}_l}{dx} = f_k,$$

where $v = r^2 (\partial \varphi / \partial x)$, and $\hat{\varphi}_k$, \hat{v}_k , and \hat{a}_k are the Fourier coefficients defined as $\varphi = \sum_{k=-N}^N \hat{\varphi}_k e^{ik\omega t}$, $v = \sum_{k=-N}^N \hat{v}_k e^{ik\omega t}$, $a = \sum_{k=-N}^N \hat{a}_k e^{ik\omega t}$. ω is the frequency of the periodic force exerted on the resonator by the shaker. The detailed expressions for $D_{kl} = D_{kl}(\hat{v}_k, \hat{\varphi}_k, x)$ and $f_k = f_k(\hat{v}_k, \hat{\varphi}_k, x)$ are given by

$$D_{kl} = (c_0^2 + ik\omega\delta) \delta_{kl} + D'_{k-l},$$

$$f_k = -k^2 \omega^2 r^2 \hat{\varphi}_k + ik\omega r^2 x \hat{a}_k + \frac{ik\omega [v^2]_k}{r^2} + \sum_{l=-N+k}^N \hat{a}_{k-l} \hat{v}_l - \frac{dr^2}{dx} \sum_{l=-N+k}^N [v^2]_{k-l} \hat{v}_l,$$

where $\delta = (\zeta + 4\eta/3)/\rho_0$ is the viscosity, $c_0 = \sqrt{\gamma p_0/\rho_0}$ is the reference speed of sound, D'_m is given by $D'_m = -(\gamma - 1)x \hat{a}_m - im\omega(\gamma - 1)\hat{\varphi}_m - [(\gamma + 1)/2r^4][v^2]_m$, and $[v^2]_k = \sum_{l=-N+k}^N \hat{v}_{k-l} \hat{v}_l$. The no-slip boundary conditions at the two ends are translated to the equivalent conditions in Fourier space: $\hat{v}_k = 0$ at $x=0, l$.

After the Fourier coefficients $\{\hat{\varphi}_k\}$ and $\{\hat{v}_k\}$ are obtained by solving the boundary-value problem, Eq. (4), the velocity potential φ and the modified velocity v are computed from the inverse FFT. The density ρ is given by the momentum equation,

$$\frac{\rho}{\rho_0} = \left(1 - \frac{\gamma - 1}{c_0^2} \left[\frac{\partial \varphi}{\partial t} + \frac{1}{2r^4} v^2 + ax - \frac{\delta}{r^2} \frac{\partial v}{\partial x} \right] \right)^{1/(\gamma - 1)}, \quad (5)$$

and the pressure p can be obtained from the state equation (3).

III. NUMERICAL METHODS

The procedures for finding the optimal shape parameters are described as follows. Given an initial resonator shape and a fixed value of maximum external force, the resonance frequency of the resonator is determined and the compression ratio, defined as the maximum-to-minimum pressure ratio at the narrow end of the cavity, is computed. Then, the optimization step is performed yielding the next resonator shape candidate. The first and the second steps are repeated until incremental changes in the resonator contour no longer produce higher compression ratios and the local optimal design is determined.

To simplify the discussion, the following dimensionless variables are introduced:

$$X = \frac{x}{l}, \quad T = \omega t, \quad R = \frac{r}{l}, \quad R_0 = \frac{r_0}{l}, \quad A = \frac{a}{l\omega_0^2}, \quad (6)$$

where ω is the frequency of the periodic force acted on the resonator, $\omega_0 = \pi c_0 / l$ is the fundamental frequency of a cylindrical resonator of length l .

In this work, the acceleration of the resonator induced by external force is assumed to be harmonic, $A(T) = \tilde{A} \cos(T)$. The physical parameters that determine the acoustic wave field in the resonator are as follows: the acceleration amplitude \tilde{A} , the ratio of specific heats γ , the attenuation coefficient $G = \pi(\zeta + 4\eta/3)\omega_0/c_0^2\rho_0$, and the resonator oscillating frequency $\Omega = \omega/\omega_0$.

A. Shape optimization

Suppose the resonator shape $R(X)$ is determined by a number of shape parameters, S_0, S_1, \dots, S_n . For example, a cone is given by $R(X) = S_0 + S_1 X$. To determine the shape producing the highest value of the pressure compression ratio R_c , i.e.,

$$R_c(S_0, S_1, \dots, S_n) = \frac{p_{\max}}{p_{\min}}, \quad \text{at } X=0, \quad (7)$$

gradients of the pressure compression ratio value are compared with the gradients of the shape parameters to indicate the next contour iteration. p_{\max} and p_{\min} denote the maximum and minimum pressure at the narrow end of the resonator during one period of oscillation, respectively. The compression ratio R_c is a function of the shape parameters, the dimensionless frequency Ω and the history of Ω (due to the existence of hysteresis effects). The method for obtaining R_c for a fixed resonator shape is explained later in the section.

The optimization method begins by specifying the practical conditions and constraints. The original experiments by Lawrenson *et al.*¹ and some commercial applications use refrigerant R-134a as the gas contained within the resonators. Therefore, the specific heat ratio $\gamma = 1.2$ is used to match the gas properties of the refrigerant. The viscosity-related parameter G is fixed at 0.010, which was found appropriate in the separate studies.^{2,7,8} The dimensionless radius of the resonator at the narrow end, $R(X=0)$, is restricted to be greater than 0.020833. This is the minimum value that would allow for a mechanical connection to the resonator required for real world applications.

Since the electrodynamic shaker system used in this study^{1,7,8} is force-limited, the resonator shape is optimized by holding constant *the maximum inertial force required to establish the periodic oscillation*. This stipulation is justified by the experimental results that the force acting on the resonator surface by the acoustic field is negligible even at resonance.⁷ This imposed constraint limits the acceleration of the resonator, \tilde{A} , and reduces \tilde{A} when additional weight is added with changing resonator geometry. Previous studies held the acceleration amplitude constant, resulting in an optimal conical resonator shape that has a very small narrow end and very large wide end.⁹ This geometry is not practical since it results in heavy weight experimental hardware. Upon application, the heavy weight resonator could not produce high compression ratios due to the low acceleration generated by the shaker system. A greater compression ratio would be obtained from lighter weight hardware oscillated at higher

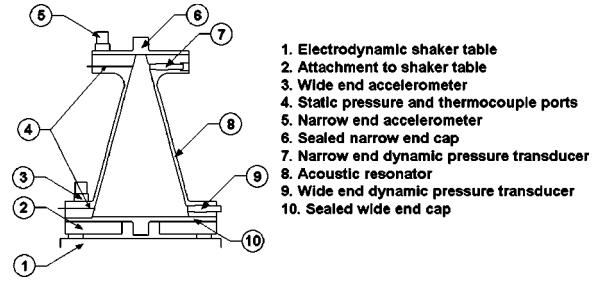


FIG. 1. Experimental apparatus.

acceleration amplitude. In this study, therefore, the maximum external force delivered to the resonator oscillation is fixed during the optimization, effectively favoring lighter weight resonators and more closely modeling the real system.

Using Newton's Second Law, for a fixed amount of maximum dimensionless external force F_{\max} , the dimensionless acceleration amplitude \tilde{A} is easily deduced from

$$\tilde{A} = F_{\max} / (M + M_a), \quad (8a)$$

where M is the dimensionless mass of the resonator given by

$$M = \int_0^1 \pi [(R(X) + D_w)^2 - R^2(X)] dX + \pi [R^2(0) + R^2(1)] D_w, \quad (8b)$$

and M_a is the mass due to the fixture and armature attached to the shaker as shown in Fig. 1. From the data in our experiments, M_a is set to the dimensionless value of 0.89295, equivalent to twice the weight of the conical resonator in our experiment. D_w is the thickness of the resonator wall nondimensionalized by the length of the resonator and is chosen to be 0.020941 matching the dimension of the conical resonator in the experiments. The second term of Eq. (8b) accounts for the mass of the two end caps of the resonator.

A quasi-Newton method, BFGS (Broyden-Fletcher-Goldfarb-Shanno),¹⁰ then is used for maximizing the multi-variable nonlinear function $R_c(S_0, S_1, \dots, S_n)$. BFGS is an iterative method, approximating the objective function by a quadratic function at each iteration. At each major iteration step, k , a line search is performed in the direction

$$d^{(k)} = H_k^{-1} \cdot \nabla R_c(S^{(k)}),$$

where $S^{(k)} = (S_0^{(k)}, S_1^{(k)}, \dots, S_n^{(k)})$ is the vector of the shape parameters at the k -th iteration of BFGS. H_k is the BFGS approximation to the Hessian matrix of R_c with respect to S , defined by

$$H_k = H_{k-1} + \frac{q_{k-1} q_{k-1}^T}{q_{k-1}^T q_{k-1}} - \frac{H_{k-1}^T t_{k-1}^T t_{k-1} H_{k-1}}{t_{k-1}^T H_{k-1} t_{k-1}},$$

where $t_{k-1} = S^{(k)} - S^{(k-1)}$, $q_{k-1} = \nabla R_c(S^{(k)}) - \nabla R_c(S^{(k-1)})$ and $H_0 = I$.

The evaluation of the objective function R_c involves solving many iterations of a nonlinear system of ODEs given in Eq. (4), since the gradient information of R_c required for the BFGS method is not available analytically. Using a numerical differentiation method via finite differences, the gra-

dient information is determined by perturbing each design variable, S_j , in turn and calculating the rate of change in the objective function $R_c(S_0, S_1, \dots, S_n)$. For two shape parameters, the optimization takes 4 to 48 hours of CPU time (depending on the type of the resonator shape and initial guess for the shape parameters) on a 1.3 GHz Athlon T-Bird PC with the Lahey-Fujitsu FORTRAN compiler.

B. Boundary value problem

For a given shape of the resonator, the boundary value problem, Eq. (4), is solved numerically by a Multiple Shooting Method. Since the amplitude of the pressure in a resonator strongly depends on the oscillating frequency Ω , the quantity to be optimized is the maximum pressure compression ratio R_c over the entire range of Ω for a given resonator shape. Because of the hysteresis effects, the solution is *not* unique near the resonance frequency and the Multiple Shooting Method will not converge unless a good initial guess of the solution is provided. To circumvent the difficulty, a continuation method is implemented. The system of ODEs is solved starting from a frequency Ω that is away from the resonance frequency and the solution is used as an initial guess for solving the ODEs for increased or decreased Ω . The steps are repeated until all branches of the solution for all values of Ω near the resonance is completed. The maximum ratio R_c among different values of Ω , and among the increasing and decreasing frequency branches (if hysteresis is present), is chosen as the compression ratio corresponding to the resonator contour.

IV. RESULTS

A. Experimental validation of the numerical method

While the numerical model by itself provides insight into the physics of the nonlinear acoustic standing waves in oscillating resonators, experimental verification is required to ensure the model's accuracy. Experimental conditions are used as inputs to the numerical model, and the numerical predictions are then compared to the experimental results.

The acceleration input to the numerical model is generated using measured signals from the experimental data. Recall that the model assumes that the resonator is excited using a simple sinusoidal acceleration. In addition, the resonator is assumed to be ideally rigid so that the acceleration is constant across the length of the resonator body. The arguments made in Finkbeiner *et al.*¹¹ allow the measured acceleration signals to be input to the model by isolating the fundamental acceleration harmonic as the driving function for the model.

The value for G , the effective viscosity parameter, is based in part upon the second coefficient of viscosity due to the high-pressure gradients and frequencies due to the acoustics. Previous work² assumed a value of $G=0.010$, although no justification was given for this value. To estimate this parameter, the pressure results from the numerical model are computed for several values of G , and are plotted together with the experimental data.^{8,12} A single comparison between

experimental and numerical data is presented here, but is characteristic of several comparisons.

A representative experimental configuration is shown in Fig. 1, with a resonator rigidly mounted on a Labworks ET-127 shaker system. PCB Piezotronics 353B03 accelerometers are mounted at both ends of the resonator. PCB Piezotronics dynamic pressure transducers are mounted in the side wall of the resonator at axial positions of $X=0.05$ and $X=0.95$. Thermocouples and Druck PDCR 130 static pressure transducers are mounted at the same axial positions as the dynamic pressure transducers. The dynamic pressure transducers are acceleration compensated, designed for high frequency measurements, and are incapable of measuring static pressure. The static pressure value is measured with static transducers and is combined with the dynamic measurements to complete the pressure measurement. The value of the maximum force limit, F_{\max} , adopted in this work corresponds to an electrodynamic shaker with 500 lbf maximum capacity and about 6 lbm armature and fixture.

At the acoustic resonance of the working fluid, the acceleration signals measured near the two ends have small difference in amplitude as graphed in Fig. 2. The dimensionless acceleration based on the signal measured at the wide and the narrow ends of the resonator is given by $\tilde{A}=9.76 \times 10^{-5}$ and $\tilde{A}=1.03 \times 10^{-4}$, respectively. The difference in the amplitude at the two ends is due to elasticity of the resonator. The dynamic pressure frequency response measured at the narrow end of the horn-cone resonator is displayed in Fig. 3 along with the curves which are computed for varying values of G with a dimensionless acceleration level, $\tilde{A}=1.03 \times 10^{-4}$, matching the acceleration measured at the resonator narrow end. The computational pressure amplitude is measured at the axial location of $X=0.05$. The result shows that the model over-predicts the resonance frequency of the horn-cone resonator by roughly 2.6%. However, in terms of amplitude and wave form, the model predicts the pressures generated in the resonator very well. The matching value of G is between 0.011 and 0.012 with acceleration referenced at the narrow end. A similar comparison shows, when the computed pressure frequency response curves are calculated based on the dimensionless acceleration at the wide end, $\tilde{A}=9.76 \times 10^{-5}$, the matching value of G is found to lie in (0.010, 0.011). These values of G are, for all intents and purposes, close to those assumed in previous studies.²

B. Optimal resonator shapes

In the following subsections, the results are shown from optimizing each type of resonator shapes to achieve maximum compression ratio R_c at one end of the resonators. The ratio of specific heats is held at $\gamma=1.2$ and the attenuation coefficient $G=0.01$ which is identical to the value used in Ilinskii *et al.*² and closely matching the value determined by the experiments discussed previously. The acceleration \tilde{A} for a given shape is calculated from Eq. (8), where the value of the maximum inertial force F_{\max} is deduced from that for a reference conical resonator accelerated at the amplitude $\tilde{A}=5 \times 10^{-4}$.

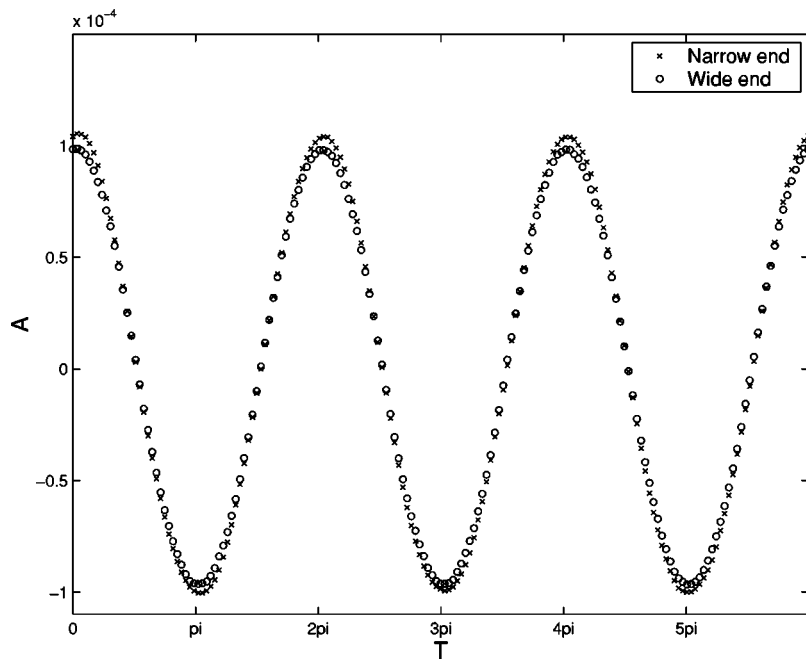


FIG. 2. The dimensionless acceleration signals measured at the two ends of the horn-cone resonator by PCB accelerometers.

1. Optimal conical shaped resonator

The conical resonator contour can be written as

$$R(X) = S_0 + S_1 X, \quad \text{for } 0 \leq X \leq 1. \quad (9)$$

The conical resonator studied in Lawrenson *et al.*¹ and Ilinkii *et al.*² with $S_0 = 0.032941$ and $S_1 = 0.26800$ is chosen to be the reference resonator, shown in Fig. 4(a). For the reference resonator, the compression ratio reaches its maximum value of $R_c = 5.0475$ when the oscillation frequency is raised to $\Omega = 1.3134$.

Using the optimization procedure described in Sec. III and starting with the reference conical shape, the optimal conical resonator is found to have the shape parameters $S_0 = 0.020833$ and $S_1 = 0.17211$. The compression ratio R_c of the conical resonator reaches a value of 5.8932, which is

about 17% higher than that of the reference resonator. Recall that, due to hysteresis, the entire branch must be traced by incrementing the frequency Ω . The compression ratio reaches the value when the frequency is increased to 1.3200. The corresponding acceleration that achieves such a compression ratio has the amplitude $\tilde{A} = 5.7470 \times 10^{-4}$. According to our assumption (8), accelerating the optimal resonator at this level requires the same amount of maximum inertial force that oscillates the reference conical resonator at $\tilde{A} = 5 \times 10^{-4}$. As stated before, to find realistic dimensions of the resonator, the optimization scheme limits the lower bound for the dimensionless radius of the resonator at the narrow end to be $R(X=0) = 0.020833$. From the dimensions of the optimal conical resonator, the smaller narrow end, S_0 , generates a larger compression ratio. Due to the fixed external

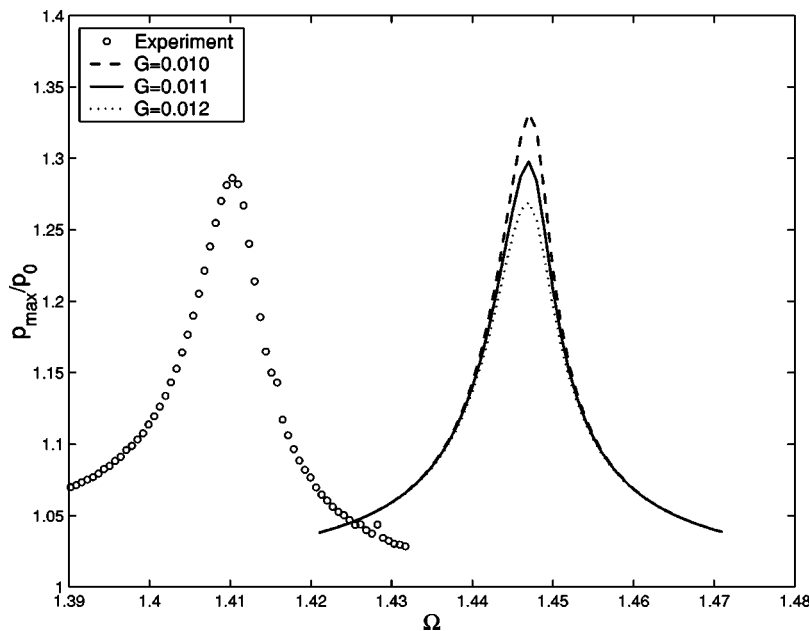


FIG. 3. The dynamic pressure frequency response measured at the narrow end of the horn-cone resonator and the pressure responses predicted by the numerical model computed for varying values of G with a dimensionless acceleration level, $\tilde{A} = 1.03 \times 10^{-4}$, matching the acceleration measured at the resonator narrow end.

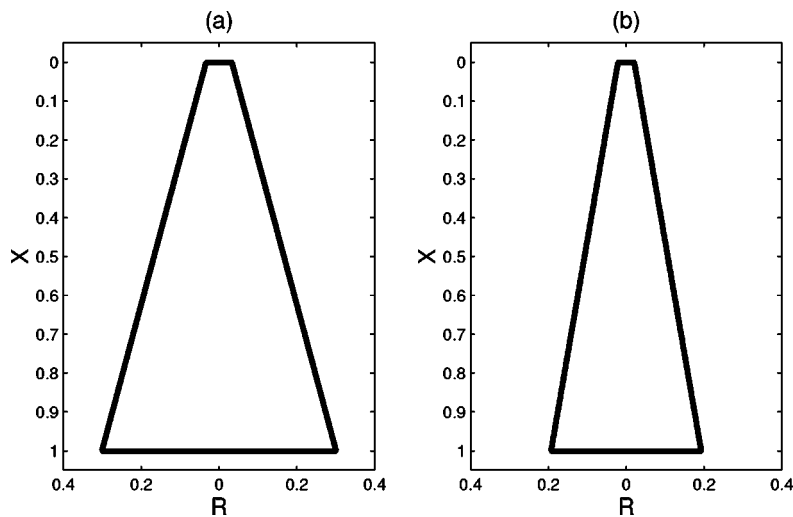


FIG. 4. Conical shapes: (a) the reference conical resonator; (b) the optimized conical resonator. For the same maximum external force, the compression ratios corresponding to the shapes in (a) and (b) reach the values of 5.0475 and 5.8932, respectively. For shape parameters, see the text.

force constraint, the slope of the optimal cone S_1 is finite. The reference resonator and the optimal conical resonator are shown in Fig. 4. The second cone [Fig. 4(b)] has a smaller narrow end and smaller slope than the reference [Fig. 4(a)].

2. Optimal horn-cone shaped resonator

The horn-cone resonator shape is described by

$$R(X) = \begin{cases} S_0 \cosh(S_1 X), & \text{for } 0 \leq X \leq S_2, \\ \alpha + \beta X, & \text{for } S_2 \leq X \leq 1, \end{cases} \quad (10)$$

where $\alpha = S_0 \cosh(S_1 S_2)$ and $\beta = S_0 S_1 \sinh(S_1 S_2)$. The three shape parameters S_0 , S_1 and S_2 are optimized. The first optimization attempt starts with the dimensions of the horn-cone given in Lawrenson *et al.*,¹ $S_0 = 0.028333$, $S_1 = 5.7264$ and $S_2 = 0.25$ [shown in Fig. 5(a)]. Using these original shape parameters, the compression ratio $R_c = 14.059$ is achieved when the horn-cone resonator is accelerated at $\tilde{A} = 5.1516 \times 10^{-4}$ and the frequency is increased to $\Omega = 1.4678$. In searching for the optimal horn-cone design, the lower bound of the radius of the narrow end S_0 is limited to be 0.020833 for practical reasons. The separation point between the horn section and the cone section, S_2 , could be any value between 0 and 1. The result of optimization finds that the compression ratio reaches a maximum value of 19.115, which is 36% higher than that of the horn-cone of Lawrenson *et al.*,¹ when the shape has $S_0 = 0.20833$, $S_1 = 5.7044$ and $S_2 = 0.25246$. This optimal horn-cone achieves the value of the compression ratio when its acceleration has the amplitude $\tilde{A} = 5.6730 \times 10^{-4}$ and it is oscillating at its resonance frequency $\Omega = 1.4716$. The value of the acceleration satisfies the requirement of fixed inertial force F_{\max} formulated in Eq. (8). For horn-cone shapes, the principle that higher compression ratio is obtained with smaller narrow end is valid, as in the case of conical shapes.

The optimization scheme BFGS is designed for finding a local extreme of a multivariable function. Our numerical simulations indicate that the compression ratio, as a function of the shape parameters, usually has many local extrema. Our second optimization attempt started with a different initial geometry of the horn-cone and a substantially larger

value of the compression ratio $R_c = 47.975$ is obtained when the shape parameters are $S_0 = 0.020833$, $S_1 = 6.1698$ and $S_2 = 0.27704$ [shown in Fig. 5(b)]. For this compression ratio, the resonator is oscillated at the acceleration amplitude $\tilde{A} = 5.1814 \times 10^{-4}$ and the frequency $\Omega = 1.5603$. Comparing with the compression ratio for the horn-cone in Lawrenson *et al.*,¹ the second optimal horn-cone improves the compression ratio by *more than 241%* at the same value of F_{\max} . Comparing the dimensions of the two horn-cones, the volumes of the shapes are similar but the optimal horn-cone has a relatively shorter cone section than that of the horn-cone used in Lawrenson *et al.*¹ In Fig. 5(c), the pressure waveform at the narrow end is presented for both the Lawrenson and the optimized horn-cone resonators. The two pressure waves

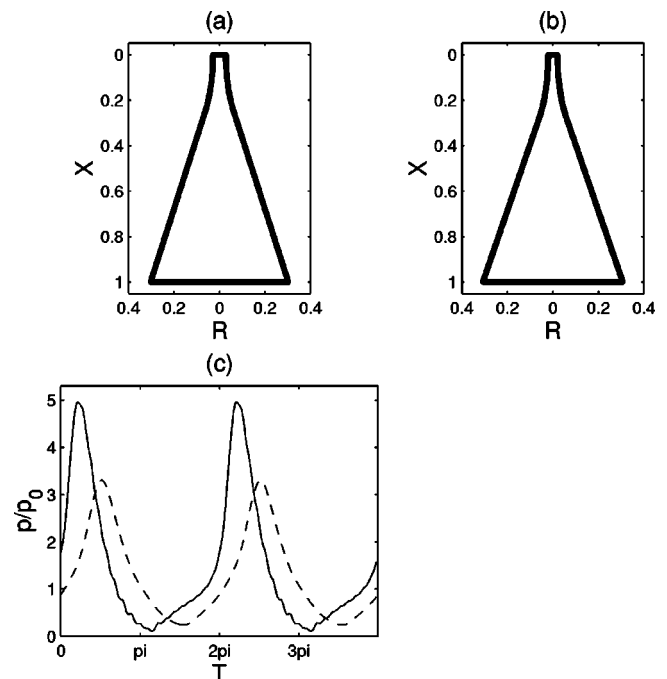


FIG. 5. (a) The horn-cone shape in Lawrenson *et al.* (Ref. 1). (b) Optimized horn-cone shape. For shape parameters, see the text. (c) The pressure waveform at the narrow end for the horn-cone in Lawrenson *et al.* (Ref. 1) (the dashed line) and that for the second optimized horn-cone (the solid line) are shown.

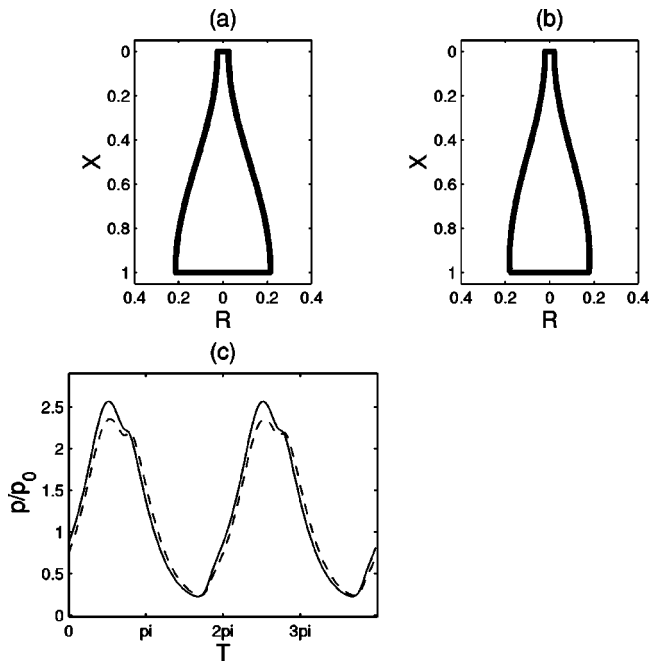


FIG. 6. (a) The $\frac{1}{2}$ -cosine shape as in Chun and Kim (Ref. 5). (b) The optimized cosine shape. (c) The pressure waveform at the narrow end for the $\frac{1}{2}$ -cosine resonator in Chun and Kim (Ref. 5) (the dashed line) and that for the optimized cosine shape (the solid line) are shown.

corresponding to the two horn-cone resonators also have different phases. Under the prescribed conditions, the peak of the pressure is about 5.0 times the ambient pressure in the optimal horn-cone while the peak is about 3.3 times for the horn-cone in Lawrenson *et al.*¹

3. Optimal cosine shaped resonator

The cosine shape is defined as

$$R(X) = S_0 + S_1(1 - \cos(S_2 X)), \quad \text{for } 0 \leq X \leq 1. \quad (11)$$

Assuming that the input power is entirely determined by the interior gas pressure, Chun and Kim⁵ compared three individual resonators of the same volume: one conical shape, one $\frac{1}{2}$ -cosine shape ($S_2 = \pi$) and one $\frac{3}{4}$ -cosine shape ($S_2 = 3\pi/2$). They found that the $\frac{1}{2}$ -cosine resonator produces the highest compression ratio among the three resonators.

Imposing our optimization constraint of external force-limit, for the $\frac{1}{2}$ -cosine dimensions reported in Chun and Kim,⁵ $S_0 = 0.025$, $S_1 = 0.095$, $S_2 = \pi$, the compression ratio reaches the value 11.216 when $\bar{A} = 5.5775 \times 10^{-4}$ and $\Omega = 1.4834$. Starting with this shape, the resulting optimal cosine shape parameters are given by $S_0 = 0.020833$, $S_1 = 0.10462$ and $S_2 = 3.2490$, and the corresponding compression ratio increases to $R_c = 11.865$ at the acceleration $\bar{A} = 5.4680 \times 10^{-4}$ and the frequency $\Omega = 1.5552$, which is about 6% better than that of Chun and Kim⁵ at the same level of force-limit. Using different initial guesses of the shape parameters for cosine resonators, the optimization scheme produced results that yielded a higher compression ratio of $R_c = 11.954$, 7% higher than that of Chun and Kim.⁵ The higher performance is achieved at $\bar{A} = 5.9209 \times 10^{-4}$ and $\Omega = 1.4837$ when the cosine resonator described by Eq. (11) has the following shape parameters: $S_0 = 0.020833$, $S_1 = 0.070327$ and $S_2 = 3.3553$. The shape is displayed in Fig. 6(b). As shown in Fig. 6(c), the pressure waveform of the optimal cosine design is smoother compared to that of Chun and Kim⁵ with a greater pressure peak and a different phase.

Under the specified conditions (the same force-limit F_{\max} , the ratio of specific heats γ and the viscosity-related parameter G), the horn-cone shape is found to be better than the cosine shape in generating higher compression ratio at the narrow end, different than the findings of Chun and Kim⁵ under a different set of criteria. The resonance frequency of the optimal horn-cone shape $\Omega = 1.5603$ is higher than that of the optimal cosine shape $\Omega = 1.4837$, and the acceleration amplitudes for achieving the corresponding compression ratios are comparable: $\bar{A} = 5.1814 \times 10^{-4}$ for the horn-cone resonator and $\bar{A} = 5.9209 \times 10^{-4}$ for the cosine resonator.

V. CONCLUSIONS

A local optimization scheme is presented for determining the axisymmetric resonator contours that maximize the pressure compression ratio at one end of an oscillating acoustic resonator. The optimal dimensions under a limiting constraint of external periodic force are reported for cone, horn-cone, and cosine shaped resonators. The results are summarized in Table I, including the shape parameters, corresponding acceleration amplitude, resonance frequency, and compression ratio.

TABLE I. A summary of the shape parameters and compression ratios of previous studies compared with the optimum geometries. For reference, the corresponding acceleration levels and fundamental resonance frequency are listed.

	S_0	S_1	S_2	$\bar{A} (\times 10^{-4})$	Ω	R_c
Cone:						
Ilinskii <i>et al.</i> (Ref. 2)	0.032941	0.26800	N/A	5.0000	1.3134	5.0475
Optimal	0.020833	0.17211	N/A	5.7470	1.3200	5.8932
Horn-cone:						
Lawrenson <i>et al.</i> (Ref. 1)	0.028333	5.7264	0.25	5.1516	1.4678	14.059
Optimal	0.020833	6.1698	0.27704	5.1814	1.5603	47.975
Cosine-shape:						
Chun and Kim (Ref. 5)	0.025	0.095	3.1416	5.5775	1.4834	11.216
Optimal	0.020833	0.070327	3.3553	5.9209	1.4837	11.954

For each type of resonator, a smaller narrow end is found to give a larger pressure peak-to-peak ratio. This finding suggests that the number of shape parameters in an optimization can be reduced by holding the diameter of the narrow end fixed at a value as small as practical. For the types of horncone and cosine shapes, there are many different designs that achieve local extrema. However, using different initial guesses a more global optimum can be determined and a 241% improvement of in compression ratio can be achieved. For the shapes considered herein, the horncone shape is found to generate the highest compression ratio. The acoustic field in a resonator is a continuous function of the resonator shape, the ratio of specific heats and the viscosities. Consequently, the dimensions of optimal resonator shape reported herein will undergo change as the specific heats and/or the viscosities change. The optimized shapes depend on the capacity and the fixture/armature mass of the force-limited shaker, the mass of the resonator, and other possible constraints that a particular application demands.

The quasi-one-dimensional model in this paper does not include the possible effects due to the boundary layer along the resonator wall and acoustically generated turbulence at high amplitudes. Nevertheless, a direct comparison is made between the results from our model and those from Ilinskii *et al.*³ which include both of these effects. We find that, for the horncone studied in Ilinskii *et al.*,³ the combined influence of the boundary layer attenuation and possible turbulence on the acoustical field, in particular, on the compression ratio of the pressure wave, is small (less than 5%) at $\tilde{A} = 5 \times 10^{-4}$, approximately the highest acceleration level considered in this paper.

- ¹C. C. Lawrenson, B. Lipkens, T. S. Lucas, D. K. Perkins, and T. W. Van Doren, "Measurements of macrosonic standing waves in oscillating closed cavities," *J. Acoust. Soc. Am.* **104**, 623–636 (1998).
- ²Y. A. Ilinskii, B. Lipkens, T. S. Lucas, T. W. Van Doren, and E. A. Zabolotskaya, "Nonlinear standing waves in an acoustical resonator," *J. Acoust. Soc. Am.* **104**, 2664–2674 (1998).
- ³Y. A. Ilinskii, B. Lipkens, and E. A. Zabolotskaya, "Energy losses in an acoustical resonator," *J. Acoust. Soc. Am.* **109**, 1859–1870 (2001).
- ⁴M. F. Hamilton, Y. A. Ilinskii, and E. A. Zabolotskaya, "Linear and nonlinear frequency shifts in acoustical resonators with varying cross sections," *J. Acoust. Soc. Am.* **110**, 109–119 (2001).
- ⁵Y.-D. Chun and Y.-H. Kim, "Numerical analysis for nonlinear resonant oscillations of gas in axisymmetric closed tubes," *J. Acoust. Soc. Am.* **108**, 2765–2774 (2000).
- ⁶R. R. Erickson and B. T. Zinn, "Modeling of finite amplitude acoustic waves in closed cavities using the Galerkin method," *J. Acoust. Soc. Am.* **113**, 1863–1870 (2003).
- ⁷J. Finkbeiner, "Nonlinear acoustic standing waves in oscillating closed containers," Master's thesis, Illinois Institute of Technology, May 2003.
- ⁸C. Daniels, J. Finkbeiner, B. Steinetz, X. Li, and G. Raman, "Determination of dimensionless attenuation coefficient in shaped resonators," presentation 4aPAa3, *145th Meeting of the Acoustical Society of America*, May 2003, Nashville, TN.
- ⁹X. Li, J. Finkbeiner, G. Raman, C. Daniels, and B. Steinetz, "Nonlinear resonant oscillations of gas in optimized acoustical resonators and the effect of central blockage," *41st AIAA Aerospace Sciences Meeting and Exhibit*, AIAA Paper No. 2003-0368, 2003, Reno, Nevada.
- ¹⁰P. E. Gill, W. Murray, and M. H. Wright, *Practical Optimization* (Academic, New York, 1981).
- ¹¹J. Finkbeiner, X. Li, C. Daniels, G. Raman, and B. Steinetz, "Effect of forcing function on nonlinear acoustic standing waves," presentation 4aPAa2, *145th Meeting of the Acoustical Society of America*, May 2003, Nashville, TN.
- ¹²C. Daniels, J. Finkbeiner, B. Steinetz, X. Li, and G. Raman, "Nonlinear oscillations and flow of gas within closed and open conical resonators," *American Institute of Aeronautics and Astronautics 42st Aerospace Sciences Meeting*, AIAA-2004-0677, Reno, Nevada, 2004, and NASA TM-2004-212902.